



# Forecasting Scrub Typhus Cases in Eight High-Risk Counties in China: Evaluation of Time-Series Model Performance

Junyu He<sup>1,2</sup>, Xianyu Wei<sup>3</sup>, Wenwu Yin<sup>4</sup>, Yong Wang<sup>3</sup>, Quan Qian<sup>3</sup>, Hailong Sun<sup>3</sup>, Yuanyong Xu<sup>3</sup>, Ricardo J. Soares Magalhaes<sup>5,6</sup>, Yuming Guo<sup>7</sup> and Wenyi Zhang<sup>3\*</sup>

<sup>1</sup>Ocean Academy, Zhejiang University, Zhoushan, China, <sup>2</sup>Ocean College, Zhejiang University, Zhoushan, China, <sup>3</sup>Chinese PLA Center for Disease Control and Prevention, Beijing, China, <sup>4</sup>Chinese Center for Disease Control and Prevention, Beijing, China, <sup>5</sup>Spatial Epidemiology Laboratory, School of Veterinary Science, The University of Queensland, Brisbane, QLD, Australia, <sup>6</sup>Child Health Research Center, The University of Queensland, Brisbane, QLD, Australia, <sup>7</sup>Department of Epidemiology and Preventive Medicine, School of Public Health and Preventive Medicine, Monash University, Melbourne, VIC, Australia

## OPEN ACCESS

### Edited by:

Sen Li,

Huazhong University of Science and Technology, China

### Reviewed by:

Olusegun Steven Ayodele Oluwole,  
University of Ibadan, Nigeria

Xiong Zhou,  
Beijing Normal University, China

### \*Correspondence:

Wenyi Zhang  
zwy0419@126.com

### Specialty section:

This article was submitted to  
Interdisciplinary Climate Studies,  
a section of the journal  
Frontiers in Environmental Science

**Received:** 27 September 2021

**Accepted:** 13 December 2021

**Published:** 12 January 2022

### Citation:

He J, Wei X, Yin W, Wang Y, Qian Q, Sun H, Xu Y, Soares Magalhaes RJ, Guo Y and Zhang W (2022) Forecasting Scrub Typhus Cases in Eight High-Risk Counties in China: Evaluation of Time-Series Model Performance. *Front. Environ. Sci.* 9:783864. doi: 10.3389/fenvs.2021.783864

Scrub typhus (ST) is expanding its geographical distribution in China and in many regions worldwide raising significant public health concerns. Accurate ST time-series modeling including uncovering the role of environmental determinants is of great importance to guide disease control purposes. This study evaluated the performance of three competing time-series modeling approaches at forecasting ST cases during 2012–2020 in eight high-risk counties in China. We evaluated the performance of a seasonal autoregressive-integrated moving average (SARIMA) model, a SARIMA model with exogenous variables (SARIMAX), and the long–short term memory (LSTM) model to depict temporal variations in ST cases. In our investigation, we considered eight environmental variables known to be associated with ST landscape epidemiology, including the normalized difference vegetation index (NDVI), temperature, precipitation, atmospheric pressure, sunshine duration, relative humidity, wind speed, and multivariate El Niño/Southern Oscillation index (MEI). The first 8-year data and the last year data were used to fit the models and forecast ST cases, respectively. Our results showed that the inclusion of exogenous variables in the SARIMAX model generally outperformed the SARIMA model. Our results also indicate that the role of exogenous variables with various temporal lags varies between counties, suggesting that ST cases are temporally non-stationary. In conclusion, our study demonstrates that the approach to forecast ST cases needed to take into consideration local conditions in that time-series model performance differed between high-risk areas under investigation. Furthermore, the introduction of time-series models, especially LSTM, has enriched the ability of local public health authorities in ST high-risk areas to anticipate and respond to ST outbreaks, such as setting up an early warning system and forecasting ST precisely.

**Keywords:** scrub typhus, time-series modeling, SARIMAX model, LSTM model, China, environmental factors, SARIMA model

## INTRODUCTION

Scrub typhus (ST) is a mite-borne disease caused by the *Orientia tsutsugamushi* (*O. tsutsugamushi*). A number of rodent species have been identified to carry *O. tsutsugamushi* including *Apodemus agrarius*, *Micromys minutus*, *Mus musculus*, *Rattus norvegicus*, *Microtus fortis*, and *Tscherskia triton* (Kim et al., 2010; O'Guinn et al., 2010; Sames et al., 2010). Once infected, patients will have typical clinical symptoms, such as fever, headache, fatigue, myalgia, chills, eschar, facial flushing, rash, acute hearing loss, and pneumonitis (Premaratna et al., 2006; Zhang et al., 2010). Delays in diagnosis of scrub typhus can lead to acute respiratory distress syndrome, septic shock, and multi-organ failure, leading to death (Chrispal et al., 2010). Currently, ST attracts considerable public health concerns in China, South Korea, India, and Thailand (Park, 2016; Rodkvamtook et al., 2018; Zheng et al., 2019). In China, not only the incidence of reported ST cases has significantly increased from 0.09 to 1.6 per 100,000 population in 2006 and 2016, respectively, but also ST cases are reported in the entire country within rural and urban communities (Li et al., 2020).

ST epidemiology has been extensively studied in China, such as identification of zoonotic sources of ST infection (Kuo et al., 2015), the clinical manifestations of ST infection (Zhang et al., 2010; 2012), the local spatial or spatio-temporal distributions of ST notifications (Kuo et al., 2011; Ding et al., 2012b), and the associations between the environmental factors and ST notifications (Tsai and Yeh, 2013; Wardrop et al., 2013; Li et al., 2014; Yang et al., 2014). Although the spatial variation of ST cases in China has been comprehensively studied, to date there are relatively few studies aiming to validate epidemiological time-series models to forecast ST cases. Precise forecasting of the ST cases can help local health administrative departments release an early warning of the increased risk of ST incidence and distribute reasonable medical resources in a timely manner for preventing and controlling the ST spread. Machine learning techniques have been developing rapidly during the past decade; random forest, support vector machine, or gradient boost machine techniques are used to determine the relationship between the studied natural attribute and the related environmental variable in the field of public health (Carvajal et al., 2018; He et al., 2018a). However, these methodologies have certain limitations on forecasting the disease in the future. The available literature indicates that several time-series modeling approaches have been applied to infectious diseases in China including the autoregressive-integrated moving average (ARIMA) model and the seasonal ARIMA (SARIMA) model (Ding et al., 2012a; Yang et al., 2015). While the ARIMA and SARIMA modeling approaches cannot account for the effect of disease-related environmental factors (e.g., the meteorological and land cover factors), the SARIMAX model allows time-variant exogenous variables to be considered along with the temporal autocorrelation in disease counts. The SARIMAX models have previously been utilized to model the time series of hemorrhagic fever with renal syndrome in China (He et al., 2018b). Recently, a new time-series modeling approach based on recurrent neural

networks (RNNs) has been developed (Yu et al., 2019; Sherstinsky, 2020). This modeling approach known as the long-short term memory (LSTM) model, a machine learning method, has shown strong ability for COVID-19 time-series forecasting (Chimmula and Zhang, 2020). The memory capability of LSTM to retain information from previous time instants is suitable for time-series forecasting, especially in the case of time-series with temporal correlations. The LSTM model inherits all features from RNN and the basic artificial neural network (ANN), such as self-learning, self-adaption, and self-organization; moreover, the structure of LSTM can to some extent solve the issue of vanishing and/or exploding temporal gradients that occur in RNN modeling (Gonzalez and Yu, 2018; DiPietro and Hager, 2020). However, to date the relative performance of these time-series modeling approaches at forecasting the time series of ST cases in high-risk areas in China has not been explored. Therefore, such a study will benefit the public health managers on providing precise ST forecasting models, especially in the high-risk ST counties.

In this study, we aimed to evaluate the performance of three competing time-series modeling approaches at uncovering the temporal variability of ST cases in eight high-risk counties of China and quantifying the role of ST-related environmental factors at explaining the temporal variation in ST incidence.

## MATERIALS AND METHODS

### Data Collection and Pre-Processing

Monthly ST cases were collected for the top eight high-risk ST counties of China for the 2012–2020 period from the China Information System for Disease Control and Prevention, including Yingshang County (Anhui province), Guangning County (Guangdong province), Huaiji County (Guangdong province), Yingde City (Guangdong province), Longling County (Yunnan province), Gengma County (Yunnan province), Mang city (Yunnan province), and Yingjiang County (Yunnan province), as shown in **Figure 1**. The total cases of the eight counties over the time period of analysis were 2,177, 2,832, 3,395, 2,688, 4,052, 1,936, 1,952, and 2,073, respectively. The criteria for a confirmed ST case included epidemiological exposure patient histories (travel to an epidemic area and contact with chiggers or rodents within 3 weeks before the onset of illness), clinical manifestations (for example, skin rash, lymphadenopathy, high fever, and eschar or ulcers), and also positivity for at least one of the laboratory diagnostic criteria/tests: isolation of *O. tsutsugamushi* from clinical specimens, or detection of *O. tsutsugamushi* by polymerase chain reaction (PCR) in clinical specimens, or a 4-fold or greater rise in serum IgG antibody titers between acute and convalescent sera by using indirect immunofluorescence antibody assay (IFA) (Zhang et al., 2013; Li et al., 2020).

Environmental data used in this study included raster maps of the normalized difference vegetation index (NDVI) representing the amount of vegetation at specific locations which was collected from the MODIS-Terra products (MOD13A2, <https://modis.gsfc>).

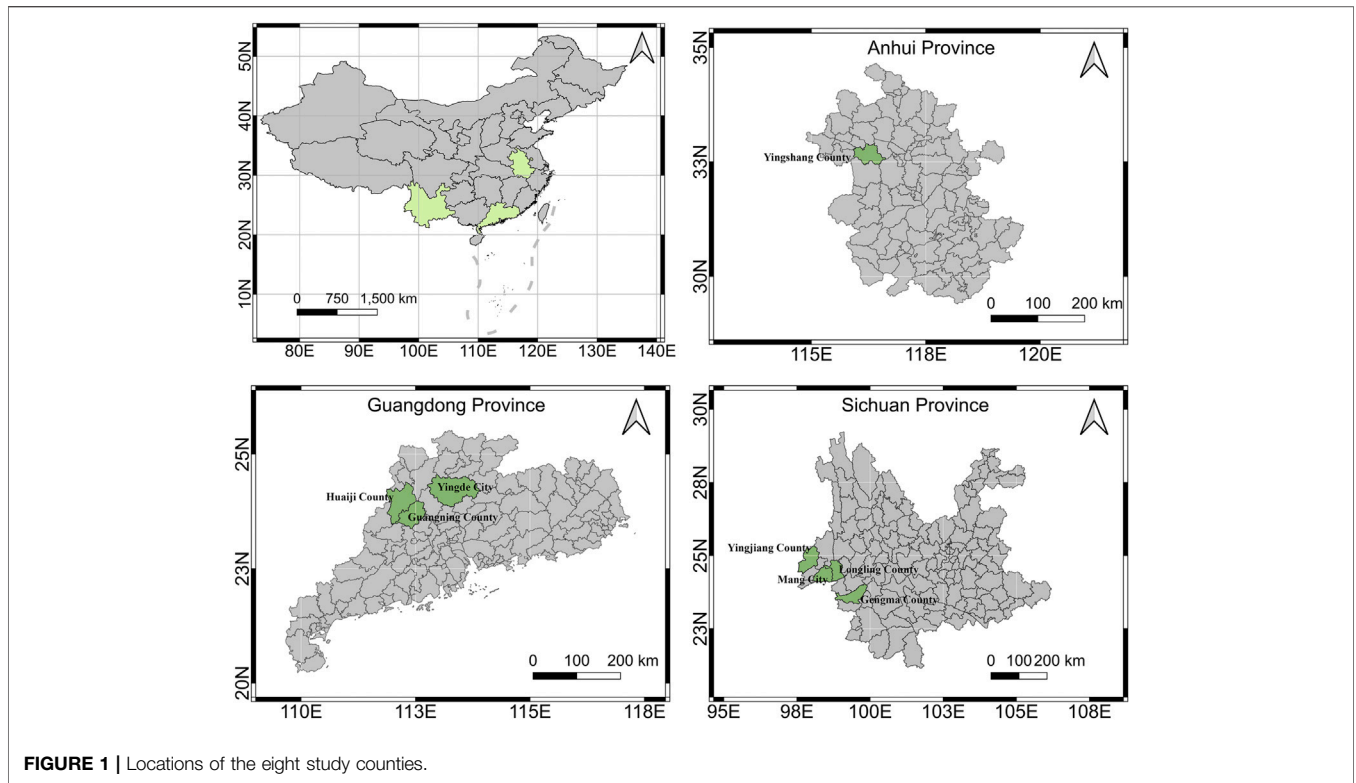


**FIGURE 1** | Locations of the eight study counties.

nasa.gov/data/dataproduct/mod13.php) with spatial resolution 1 km. We also used meteorological data from weather monitoring stations in China from the China Meteorological Administration (<http://www.cma.gov.cn/>), including precipitation, pressure, relative humidity, sunshine duration, daily mean temperature, daily minimum temperature, daily maximum temperature, and mean wind speed. The multivariate El Niño/Southern Oscillation Index (MEI), regarded as global climate change proxy, was collected from the physical sciences laboratory of National Oceanic and Atmospheric Administration (<https://psl.noaa.gov/enso/mei/>).

The inverse distance weighted method was employed for mapping the six meteorological data with the same spatial resolution of the NDVI. Then, the NDVI and the six meteorological data were extracted by the administrative boundaries of the eight counties, and the mean values of each variable were calculated each month during the study period for further analysis.

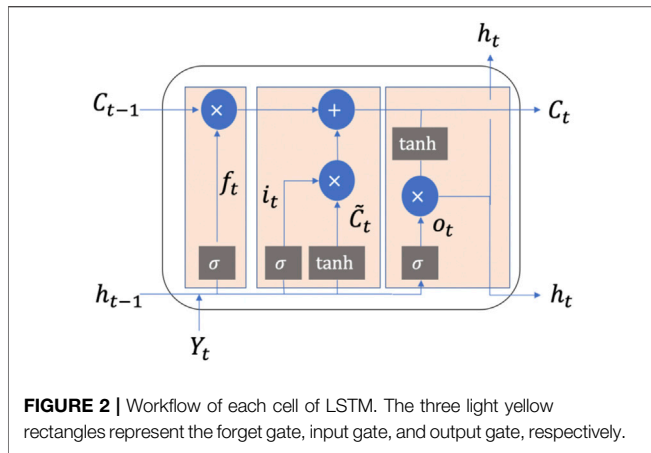
### SARIMAX Modeling

Based on the standard ARIMA model, the SARIMAX model considers simultaneously the seasonal variation in ST cases and accounts for the effects of exogenous risk factors for better understanding and fitting the considered time series. The basic equations of SARIMAX are as follows:

$$Y_t = \sum \beta_i X_{i,t} + Z_t, \tag{1}$$

$$\Phi_P(B^S)\phi_p(B)\nabla_S^D\nabla^d Z_t = \Theta_Q(B^S)\theta_q(B)\varepsilon_t, \tag{2}$$

where  $Y_t$  represents the ST cases at time instant  $t$ , while  $X_{i,t}$  represents the  $i^{th}$  exogenous variables ( $i = 1, 2, \dots, 8$ ) at time instant  $t$ , and  $\beta_i$  represent the coefficients of the exogenous variables;  $Z_t$  representing the main trend of the ST time series satisfies the SARIMA equation (Eq. 2) based on the model structure  $(p, d, q) \times (P, D, Q)_S$ . In Eq. 2,  $S$  represents the periodicity, and  $\varepsilon_t$  denotes the white noise;  $B$  represents the backshift operator, e.g.,  $B^i Z_t = Z_{t-i}$ , while  $\nabla$  represents the differencing process, e.g.,  $\nabla^d = (1 - B)^d$ ,  $\nabla_S^D = (1 - B^S)^D$  with the non-seasonal and seasonal differencing orders  $d$  and  $D$ , respectively;  $\phi_p(B) = 1 - \sum_{i=1}^p \phi_i B^i$  and  $\Phi_P(B^S) = 1 - \sum_{i=1}^P \Phi_i B^{iS}$  represent the non-seasonal and seasonal autoregressive process with the orders  $p$  and  $P$ , respectively;  $\theta_q(B) = 1 - \sum_{i=1}^q \theta_i B^i$  and  $\Theta_Q(B^S) = 1 - \sum_{i=1}^Q \Theta_i B^{iS}$  represent the non-seasonal and seasonal moving average processes with the orders  $q$  and  $Q$ , respectively. In the current study, the periodicity parameter  $S$  was set to 12 months. The main procedure of defining the structure of SARIMAX is briefly described as follows: 1) SARIMA models with the parameters  $p, P, q,$  and  $Q$  ranged from 0, 1, and 2, and the parameters  $d$  and  $D$  ranged from 0 and 1 were constructed to fit the time series of ST cases in each of the eight studied counties. The model with the lowest Akaike information criterion (AIC) value was regarded as the best SARIMA model. 2) Multicollinearity was investigated before entering the exogenous variables into the SARIMAX model. We found a very high level of correlation (0.9834 and 0.9912, respectively) between mean temperature and daily minimum temperature (or daily maximum temperature), and therefore, the daily mean temperature was selected for modeling in the current study. In



our study, eight exogenous variables with a 0–5 month lag were prepared in an exogenous variable pool. Based on the SARIMA model, a forward stepwise variable selection procedure was implemented to build the SARIMAX model. During each of the variable selection loops, multicollinearity was tested before adding the exogenous variable into the model, and only the one with a variance inflation factor (VIF) smaller than 3 was regarded as a candidate. Furthermore, the variable candidates were added into the model separately, and only the one with the lowest AIC in each loop was added into the model. Finally, a  $t$ -test was used to exclude the exogenous variables with largest  $p$ -values (larger than 0.05). More detailed information can be found in the literature (He et al., 2018b). The first eight-year ST cases were employed to fit the SARIMAX model, and the last year data were used to test the performance of the built model. To evaluate the goodness of the fit of the model, we considered the  $R^2$ , mean absolute error (MAE), and root mean square error (RMSE).

## LSTM Modeling

In order to test the possibility of applying LSTM in ST modeling and forecasting, the exogenous variables included in the final SARIMAX model together with the ST time series were chosen as the LSTM input. LSTM is constructed by a number of connected cells (the basic unit of the network), while each cell consists of three gates, i.e., the forget gate, input gate, and output gate; see **Figure 2**. Specifically, the hidden state from the previous cell  $h_{t-1}$  and the current series  $Y_t$  at time instant  $t$  are combined and flow through the forget gate, leading to useless information of loss by  $f_t = \sigma(W_f \cdot [h_{t-1}, Y_t] + b_f)$ ; in other words, the forget gate can retain the useful information in series modeling. The input gate gathers the hidden state and current series to update the cell situation  $C_t$  of LSTM, and two preparation workflows are designed, i.e.,  $i_t = \sigma(W_i \cdot [h_{t-1}, Y_t] + b_i)$  and  $\tilde{C}_t = \tanh(W_C \cdot [h_{t-1}, Y_t] + b_C)$ , and the cell situation can be calculated by  $C_t = f_t * C_{t-1} + i_t * \tilde{C}_t$ ; in other words, the input gate collects and updates the information flow into the model. The output gate uses the hidden state and current series to update the hidden state as the input of the next cell of LSTM, i.e.,  $o_t = \sigma(W_o \cdot [h_{t-1}, Y_t] + b_o)$  and  $h_t = o_t * \tanh(C_t)$ ; in other words, the output gate integrates the information and generates

the output information for the next time instant. In these equations,  $\sigma$  represents the sigmoid activate function,  $W$  and  $b$  represent the weights and bias in different parts of LSTM, respectively. Other than some other advanced LSTM models, such as forward and backward variate sensitive LSTM, convolutional LSTM, and convolutional neural network LSTM (Kim and Cho, 2019; Wan et al., 2019; Fouladgar and Främling, 2020), the current study used the basic LSTM as described above to forecast the ST series. To define the best structure of the LSTM model, the values of the hidden layers were considered to vary from 2 to 3, while the hidden dimension varies from 54 to 68 with interval 4, the batch size varies from 45 to 55 with interval 5, and the number of previous months used to forecast the current month ranges from 3 to 12. The optimal model was selected with the largest  $R^2$  and smallest MAE and RMSE.

## RESULTS

### The Performance of SARIMA and SARIMAX Models on ST Forecasting

Various SARIMA and SARIMAX models were established with different model structures, and temporal lagged exogenous variables at the eight considered counties and the optimal model structure with the corresponding performance are presented in **Supplementary Appendix Table A1**. According to the optimal model structures, all models have the same seasonal difference order, i.e.,  $D = 1$ . Specifically, the models of the four counties in the Yunnan province have very similar seasonal characteristics, i.e.,  $P$ ,  $D$ , and  $Q$  are exactly the same, except the  $Q$  value for Yingjiang County. Regarding the SARIMA model, it showed good performance in modeling ST variations in the model fitting stage in Guangning County, Longling County, and Yingjiang County with  $R^2$  larger than 0.8, while the SARIMA model showed better performance (in terms of  $R^2$ ) at the model forecasting stage in Longling County, Gengma County, and the Mang city of the Yunnan province (**Table 1**).

Through exogenous variable selection processes, the SARIMAX models absorb the strength of one or several exogenous variables with temporal lags for ST variation modeling. Atmospheric pressure with a 4-month temporal lag was found to be the sole exogenous variable for SARIMAX modeling in Huaiji County. As shown in **Supplementary Appendix Table A1**, the significant ST-associated exogenous variables vary between the eight counties under investigation. Atmospheric pressure, sunshine duration, wind speed, and MEI with various temporal lags were found to be correlated with the ST temporal variation in Yingyang County and Guangning County; however, precipitation and relative humidity were also included in ST forecasting at Yingyang County, while NDVI was included in the model at Guangning County. At Gengma County and Yingjiang County, relative humidity and sunshine duration were significant variables associated with ST; specifically, mean temperature was also found to be associated with ST at Yingjiang County. In addition, mean temperature and wind speed were two important impact factors of ST at Yingde city and Mang city, but precipitation and MEI were considered as other important factors

**TABLE 1** | Performance of SARIMA, SARIMAX, and LSTM on forecasting ST cases at eighty counties of China.

County	Model	Model fitting		Model forecasting		
		R <sup>2</sup>	AIC	R <sup>2</sup>	RMSE	MAE
Yingshang County	SARIMA	0.614	133.457	-0.009	22.568	6.973
	SARIMAX	0.860	92.181	0.647	13.343	4.870
	LSTM	0.773	-	0.780	10.525	7.901
Guangning County	SARIMA	0.801	99.555	0.670	11.571	10.043
	SARIMAX	0.835	71.355	0.031	19.818	16.613
	LSTM	0.793	-	0.561	13.343	11.908
Huaiji County	SARIMA	0.794	138.789	0.638	35.676	19.997
	SARIMAX	0.802	120.790	0.596	37.690	21.142
	LSTM	0.698	-	0.475	42.941	24.302
Yingde city	SARIMA	0.692	115.595	0.409	30.612	19.369
	SARIMAX	0.705	91.884	0.272	33.950	22.172
	LSTM	0.533	-	0.411	30.538	22.013
Longling County	SARIMA	0.874	124.253	0.899	18.809	12.804
	SARIMAX	0.898	112.597	0.807	26.034	15.422
	LSTM	0.888	-	0.863	21.900	14.776
Gengma County	SARIMA	0.773	134.443	0.910	4.773	3.692
	SARIMAX	0.837	124.531	0.552	10.674	8.051
	LSTM	0.630	-	0.750	7.976	5.750
Mang city	SARIMA	0.734	149.046	0.968	6.229	4.4919
	SARIMAX	0.816	134.120	0.941	8.461	6.840
	LSTM	0.593	-	0.831	14.254	9.506
Yingjiang County	SARIMA	0.816	119.549	0.616	19.247	11.895
	SARIMAX	0.846	110.471	0.630	18.891	11.853
	LSTM	0.864	-	0.553	20.754	13.695

for the two cities, respectively. Finally, the ST variation at Longling County was closely correlated with precipitation, relative humidity, and mean temperature with various temporal lags. Compared to the SARIMA model, the results of the SARIMAX model showed that more accuracy performance (in terms of R<sup>2</sup>) can be achieved at the model fitting stage in all of the eight counties; meanwhile, at the model forecasting stage, only the SARIMAX models in Yingshang County and Yingjiang County showed better forecasting accuracy than the SARIMA models in terms of RMSE and MAE.

## ST Cases Forecast Performance of LSTM Models

By inputting the ST series and the corresponding significantly related exogenous variables shown in **Supplementary Appendix Table A1** to the LSTM model, the optimal model structure was obtained according to the smallest R<sup>2</sup> in the model fitting stage. The results showed that better performance can be yielded by setting the length of input series as 12 months at Huaiji County, Yingde city, Longling County, Gengma County, and Yingjiang County, while the optimal length of input series at Yingshang County, Guangning County, and Mang city were 10, 3, and 11, respectively. The hidden dimension, batch size, and number of layers varied between counties. At the model fitting process, the

LSTM model showed better performance than SARIMA at Yingshang County and Longling County in terms of R<sup>2</sup>; at the model forecasting stage, LSTM showed more accuracy in forecasting ST cases than SARIMA and SARIMAX at Yingshang County and Yingde County, while only than SARIMAX at Guangning County and Longling County (**Table 1**).

## The Comparisons of SARIMA, SARIMAX, and LSTM Estimations

The model fitting and forecasting results were separated by a vertical dash line, as shown in **Figure 3**. The gray line, yellow line, red line, and green line represent the real ST notification series, SARIMA estimation, SARIMAX estimation, and LSTM estimation, respectively. It can be concluded as follows: 1) the LSTM model used a smaller length of input data for ST fitting than SARIMA and SARIMAX because the green line begins much earlier than the yellow and red lines; for example, most of the green lines at the eight counties begins during 2013 except the Guangning County, while the yellow and red lines begin during 2014 for Yingshang County, Huaiji County, Yingde County, and Yingjiang County, and for the other four counties, the model estimations begin during 2015. 2) Compared to the SARIMA and SARIMAX, LSTM showed smoother estimation values and less local fluctuations. 3)

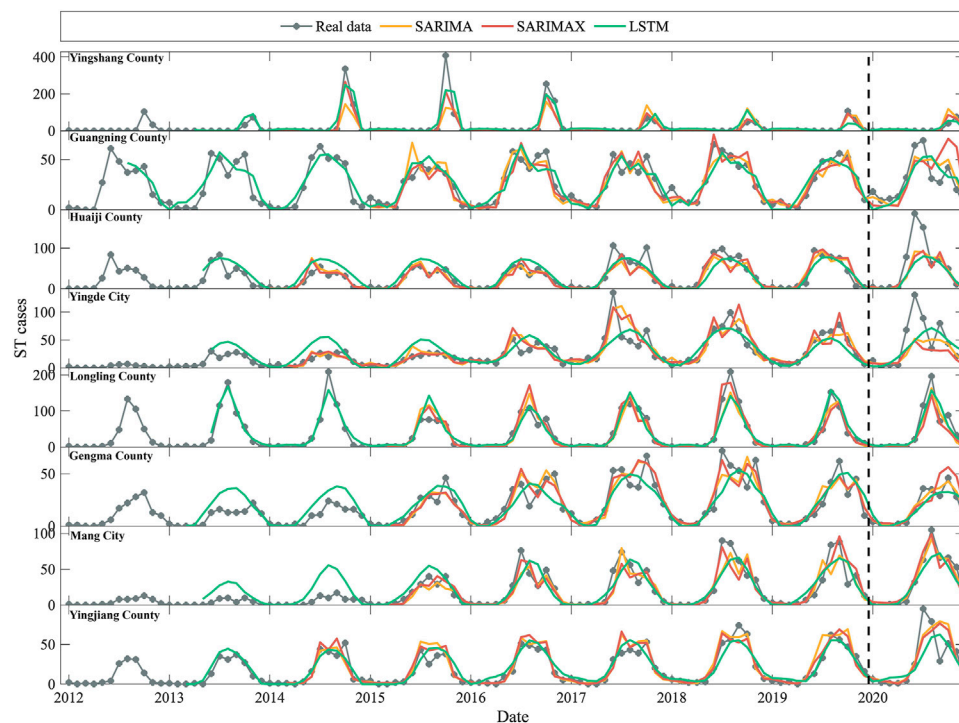


**FIGURE 3** | ST fitting and forecasting results by SARIMA, SARIMAX, and LSTM at eight counties of China. The vertical dash line separated the model fitting and forecasting parts.

Through comparing the real ST time series in the eight counties, four kinds of temporal patterns of ST variations can be concluded as follows: the ST series peaks in October and August in Yingshang County and Longling County, respectively; two peaks can be found in June and October in Guangning County, Huaiji County, and Yingde city, while in Gengma County, Mang city, and Yingjiang County, bio-peak phenomena can also be found in summer and winter during multiple years of the study period.

## DISCUSSION

### Methodological Considerations for Modeling Temporal Variation in ST Notifications

Although the performance of the three time-series forecasting methods varied between counties at both the model fitting stage and the model forecasting stage, the methodological comparisons among SARIMA, SARIMAX, and LSTM should be discussed as follows: 1) continuous series modeling was the core concept of the three methods, i.e., the previous conditions can be used to forecast the current or future conditions; furthermore, the SARIMA and SARIMAX models took a step ahead that included seasonal or cyclic parts in modeling, i.e., the seasonal auto regression part and seasonal moving average part with the cycle of 12 months. Similarly, the similar SARIMA model was employed for

modeling the ST series at Laiwu city and Shandong province, China (Ding et al., 2012a; Yang et al., 2015). On the other hand, LSTM also borrows the continuous characteristics of ST series for forecasting. Compared to the standard artificial neural network (ANN), the forget gate was utilized to remove the information with larger lags, which is similar to the memory of humans that one can remember the recent things but will forget some of the things that occurred long time ago (Yu et al., 2019). In the current work, we have demonstrated that the length of the time-series data used to forecast ST varies between high-risk counties being 12 months in five counties, 11, 10, and 3 months in the other three counties. These results indicate that ST has predominantly an annual cycle, which is in line with the literature that 8–12 months is the general cycle of ST in Guangzhou city, China (Wei et al., 2017). 2) Previous studies have used a number of regression techniques to unravel the ST temporal variation in incidence, and its associations with environmental factors using the spatial Poisson regression model, negative binomial regression model, MaxEnt, random forest, and ANN models (Wardrop et al., 2013; Li et al., 2014; Yang et al., 2014; Kwak et al., 2015; Seto et al., 2017; Yu et al., 2018; Acharya et al., 2019). However, these models cannot capture the seasonal characteristics of ST incidence, which can be overcome by the SARIMAX model that can simultaneously depict the seasonal characteristics and the effects of exogenous factors. Given the complex and often nonlinear interplay between ST factors and ST infection (Elliott et al., 2019), the linear regression component of the SARIMAX model may not be sufficient for modeling and

forecasting ST incidence. The LSTM model offers a self-organizing, self-learning, and highly nonlinearity system from the ANN, and thus, it is rather suitable for modeling the ecological system of ST. In view of its model structure, the LSTM was initially postulated as the optimal model among the three methods. However, our results indicate that LSTM not always outperforms SARIMA or SARIMAX indicating that the selection of methods for ST series modeling and forecasting should be carefully considered through model comparison and validation to local conditions.

## Environmental Factors Associated With the Temporal Variation in ST Notifications

Another outcome of the current work is the determination of environmental factors in each of the considered eight counties associated with ST cases using SARIMAX models. Including these factors (i.e., exogenous variables mentioned above), the SARIMAX showed better performance than SARIMA at the modeling fitting stage (**Table 1**), demonstrating that the considered factors were significantly associated with ST variations. Temperature with various temporal lags was found to be positively related to ST variations at Yingde city, Longling County, Mang city, and Yingjiang County, which is in line with the ecological niche modeling of ST in the literature that temperature was found to be the key factor in determining ST occurrence (Yu et al., 2018). A previous study found that the sunshine duration was negatively and positively associated with ST with 1–3 month lags and 4–6 month lags, respectively (Yang et al., 2014). Similar findings can be found in the current study, i.e., sunshine duration with 3-, 2-, and 1-month lags were negatively associated with the ST variations at Yingshang County, Guangning County, and Gengma County, respectively, but the sunshine duration with 0-month lag showed positive relationship with ST at Yingjiang County. Warming the environment promotes the growth of vector larvae and rodents and increased exposure opportunities due to people wearing shorter clothes (Yao et al., 2019). The other study found that the ST case was positively correlated with the duration of sunshine, suggesting an occupational exposure where people possibly have longer time for agricultural field work, leading to an increased probability of exposure (Li et al., 2014). Besides, relative humidity and pressure were supposed to be key factors that influenced the regeneration of the rodents, i.e., a 1–2 month lag effects of relative humidity and pressure were closely related to the ST variation (Sun et al., 2017), which is similar to the findings of the results at Yingshang County, Guangning County, Huaiji County, Longling County, and Gengma County. In our study, we considered the wind speed in our SARIMAX models with 1-, 2-, 3-, 5-month lag since it can be a factor associated with the spawning conditions of mites (Kwak et al., 2015). Indeed, we found that wind speed was a contributor to ST variation at four counties of the current study, especially in Yingde city. Finally, our results indicate a significant effect of the multivariate ENSO index on the time series of ST cases in

three of the eight counties investigated (i.e., Yingshang County, Guangning County, and Mang city). This is in line with other studies that found an association between ST incidence and the ENSO Index which is regarded as a global pattern of climatic oscillation affecting the local environment and thus human population behaviors (Wei et al., 2017).

## Contribution to Public Health

Machine learning techniques have become popular in modeling nonlinear systems, including in the field of public health (dos Santos et al., 2019; Panch et al., 2018), by providing precise predictive models (Passos et al., 2016). Introduction of LSTM has enriched the ability of local public health authorities in ST high-risk areas to anticipate and respond to ST outbreaks. The proposed models, such as SARIMAX and LSTM, can be used locally in high-risk ST counties for ST early warning and precise ST forecasting programs; it can also enable local public health managers to monitor the variation of the environmental factors and deploy public health measures, such as health promotion alerts to the communities to prevent large ST outbreaks.

## Limitations and Future Work

Certain limitations of the current work should be mentioned. First, due to lack of a longer time series of ST series data, this study only utilized a 96-month time series for model fitting, which may have hindered the performance of LSTM models; it may be the reason why LSTM showed low accuracy in ST estimation. Second, this study explored the basic LSTM model in structure and did not explore modeling combinations that considered SARIMAX + LSTM, which can also give accuracy predictions (Sheng and Jia, 2020); hence, future studies should explore the possibility of this combination for ST forecasting. Third, our SARIMAX models did not consider socioeconomic factors (including the gross domestic product, income, urbanization, population density, educational institutions, land use and land change, and medical institution), which may also play a role in the variations of ST (Ranjan and Prakash, 2018). Finally, although it is reported the warming condition might favor the reproduction of mites and increase the probability of human infection, the mechanism between the global climate change and ST outbreaks is still unclear (Jeung et al., 2016; Kuo et al., 2015); given the short-term impact of temperature mentioned in previous subsection, the long-term impact of global climate change (such as the warming condition) on ST outbreaks and its feasibility in forecasting ST outbreaks are worthy to explore in the future (Zhou et al., 2021); furthermore, the hydrology impact of climate change on ST variations will be another topic for consideration (Zhou et al., 2018).

## CONCLUSION

In the current study, SARIMA, SARIMAX, and LSTM models were employed to model the temporal variation of ST cases in

high-risk communities in China. The results indicated that annual dynamics of ST vary significantly between the eight studied counties; with exogenous variables, the SARIMAX and LSTM models showed better performance than SARIMA models. Specifically, precipitation, atmospheric pressure, relative humidity, mean temperature, sunshine duration, wind speed, NDVI, and MEI were found to be partly associated with the time series of ST cases. The models and findings of the current study will support the development of local early warning systems for ST in the high-risk areas in China.

## DATA AVAILABILITY STATEMENT

The data analyzed in this study are subject to the following licenses/restrictions: Patient data are protected by the China CDC and are unsuitable for public sharing. The scrub typhus data are not allowed to be publicly shared due to the local infection disease law. Requests to access these datasets should be directed to data@chinacdc.cn.

## REFERENCES

- Acharya, B., Chen, W., Ruan, Z., Pant, G., Yang, Y., Shah, L., et al. (2019). Mapping Environmental Suitability of Scrub Typhus in Nepal Using MaxEnt and Random Forest Models. *Int. J. Env. Res. Public Health* 16, 4845. doi:10.3390/ijerph16234845
- Carvajal, T. M., Viacrusis, K. M., Hernandez, L. F. T., Ho, H. T., Amalin, D. M., and Watanabe, K. (2018). Machine Learning Methods Reveal the Temporal Pattern of Dengue Incidence Using Meteorological Factors in Metropolitan Manila, Philippines. *BMC Infect. Dis.* 18, 183. doi:10.1186/s12879-018-3066-0
- Chimmula, V. K. R., and Zhang, L. (2020). Time Series Forecasting of COVID-19 Transmission in Canada Using LSTM Networks. *Chaos, Solitons & Fractals* 135, 109864. doi:10.1016/j.chaos.2020.109864
- Chrispal, A., Boorugu, H., Gopinath, K. G., Prakash, J. A. J., Chandy, S., Abraham, O. C., et al. (2010). Scrub Typhus: an Unrecognized Threat in South India - Clinical Profile and Predictors of Mortality. *Trop. Doct* 40, 129–133. doi:10.1258/td.2010.090452
- Ding, L., Ding, S. J., Zhang, M., Wang, X. J., Li, Z., and Zhao, Z. T. (2012a). Study on the Characteristics of Temporal Distribution and the Epidemic Trend of Autumn-winter Type Scrub Typhus under Time Series Analysis. *Zhonghua Liu Xing Bing Xue Za Zhi* 33, 698–701.
- Ding, L., Li, Z., Wang, X. J., Ding, S. J., Zhang, M., and Zhao, Z. T. (2012b). Analysis of Epidemic Features of Scrub Typhus between Year 2006 and 2010 in Shandong Province, China. *Zhonghua Yu Fang Yi Xue Za Zhi* 46, 338–342.
- DiPietro, R., and Hager, G. D. (2020). "Chapter 21 - Deep Learning: RNNs and LSTM," in *Handbook of Medical Image Computing and Computer Assisted Intervention, The Elsevier and MICCAI Society Book Series*. Editors S.K. Zhou, D. Rueckert, and G. Fichtinger (Amsterdam: Academic Press), 503–519. doi:10.1016/B978-0-12-816176-0.00026-0
- dos Santos, B. S., Steiner, M. T. A., Fenerich, A. T., and Lima, R. H. P. (2019). Data Mining and Machine Learning Techniques Applied to Public Health Problems: A Bibliometric Analysis from 2009 to 2018. *Comput. Ind. Eng.* 138, 106120. doi:10.1016/j.cie.2019.106120
- Elliott, I., Pearson, I., Dahal, P., Thomas, N. V., Roberts, T., and Newton, P. N. (2019). Scrub Typhus Ecology: A Systematic Review of Orientia in Vectors and Hosts. *Parasites Vectors* 12, 513. doi:10.1186/s13071-019-3751-x
- Fouladgar, N., and Främling, K. (2020). A Novel LSTM for Multivariate Time Series with Massive Missingness. *Sensors* 20, 2832. doi:10.3390/s20102832
- Gonzalez, J., and Yu, W. (2018). Non-Linear System Modeling Using LSTM Neural Networks. *IFAC-PapersOnLine* 51, 485–489. doi:10.1016/j.ifacol.2018.07.326

## AUTHOR CONTRIBUTIONS

JH and WZ contributed to conception and design of the study. WZ, WY, YW, and QQ organized the database. JH performed the statistical analysis. JH wrote the first draft of the manuscript. All authors contributed to manuscript revision, read, edit, and approved the submitted version.

## FUNDING

This work is partly supported by the China Postdoctoral Science Foundation (2020M681825) and the projects from the 13th Five-Year Plan (Nos.18QNP063 and 17SAZ01).

## SUPPLEMENTARY MATERIAL

The Supplementary Material for this article can be found online at: <https://www.frontiersin.org/articles/10.3389/fenvs.2021.783864/full#supplementary-material>

- He, J., Christakos, G., Wu, J., Cazelles, B., Qian, Q., Mu, D., et al. (2018a). Spatiotemporal Variation of the Association between Climate Dynamics and HFRS Outbreaks in Eastern China during 2005–2016 and its Geographic Determinants. *Plos Negl. Trop. Dis.* 12, e0006554. doi:10.1371/journal.pntd.0006554
- He, J., Yin, W., He, J., Han, Z., Teng, Y., and Zhang, W. (2018b). Environmental Determinants of Hemorrhagic Fever with Renal Syndrome in High-Risk Counties in China: A Time Series Analysis (2002–2012). *Am. J. Trop. Med. Hyg.* 99, 1262–1268. doi:10.4269/ajtmh.18-0544
- Jeung, Y. S., Kim, S.-W., Kim, D.-M., Yun, N. R., Han, M. A., and Kim, C.-M. (2016). Effect of Latitude and Seasonal Variation on Scrub Typhus, South Korea, 2001–2013. *Am. J. Trop. Med. Hyg.* 94, 22–25. doi:10.4269/ajtmh.15-0474
- Kim, T.-Y., and Cho, S.-B. (2019). Predicting Residential Energy Consumption Using CNN-LSTM Neural Networks. *Energy* 182, 72–81. doi:10.1016/j.energy.2019.05.230
- Kim, H. C., Lee, I. Y., Chong, S. T., Richards, A. L., Gu, S. H., Song, J.-W., et al. (2010). Serosurveillance of Scrub Typhus in Small Mammals Collected from Military Training Sites Near the DMZ, Northern Gyeonggi-Do, Korea, and Analysis of the Relative Abundance of Chiggers from Mammals Examined. *Korean J. Parasitol.* 48, 237–243. doi:10.3347/kjpp.2010.48.3.237
- Kuo, C.-C., Huang, J.-L., Ko, C.-Y., Lee, P.-F., and Wang, H.-C. (2011). Spatial Analysis of Scrub Typhus Infection and its Association with Environmental and Socioeconomic Factors in Taiwan. *Acta Tropica* 120, 52–58. doi:10.1016/j.actatropica.2011.05.018
- Kuo, C.-C., Lee, P.-L., Chen, C.-H., and Wang, H.-C. (2015). Surveillance of Potential Hosts and Vectors of Scrub Typhus in Taiwan. *Parasites Vectors* 8, 611. doi:10.1186/s13071-015-1221-7
- Kwak, J., Kim, S., Kim, G., Singh, V., Hong, S., and Kim, H. (2015). Scrub Typhus Incidence Modeling with Meteorological Factors in South Korea. *Int. J. Env. Res. Public Health* 12, 7254–7273. doi:10.3390/ijerph120707254
- Li, T., Yang, Z., Dong, Z., and Wang, M. (2014). Meteorological Factors and Risk of Scrub Typhus in Guangzhou, Southern China, 2006–2012. *BMC Infect. Dis.* 14, 139. doi:10.1186/1471-2334-14-139
- Li, Z., Xin, H., Sun, J., Lai, S., Zeng, L., Zheng, C., et al. (2020). Epidemiologic Changes of Scrub Typhus in China, 1952–2016. *Emerg. Infect. Dis.* 26, 1091–1101. doi:10.3201/eid2606.191168
- O'Guinn, M. L., Klein, T. A., Lee, J. S., Richards, A. L., Kim, H.-C., Ha, S. J., et al. (2010). Serological Surveillance of Scrub Typhus, Murine Typhus, and



- Leptospirosis in Small Mammals Captured at Firing Points 10 and 60, Gyeonggi Province, Republic of Korea, 2001-2005. *Vector-Borne Zoonotic Dis.* 10, 125–133. doi:10.1089/vbz.2008.0123
- Panch, T., Szolovits, P., and Atun, R. (2018). Artificial Intelligence, Machine Learning and Health Systems. *J. Glob. Health* 8, 020303. doi:10.7189/jogh.08.020303
- Park, J. (2016). Recent Outbreak of Scrub Typhus in North Western Part of India. *Indian J. Med. Microbiol.* 34, 114. doi:10.4103/0255-0857.167682
- Passos, I. C., Mwangi, B., and Kapczynski, F. (2016). Big Data Analytics and Machine Learning: 2015 and Beyond. *The Lancet Psychiatry* 3, 13–15. doi:10.1016/s2215-0366(15)00549-0
- Premaratna, R., Chandrasena, T. G. A. N., Dassayake, A. S., Loftis, A. D., Dasch, G. A., and de Silva, H. J. (2006). Acute Hearing Loss Due to Scrub Typhus: A Forgotten Complication of a Reemerging Disease. *Clin. Infect. Dis.* 42, e6–8. doi:10.1086/498747
- Ranjan, J., and Prakash, J. A. J. (2018). Scrub Typhus Re-Emergence in India: Contributing Factors and Way Forward. *Med. Hypotheses* 115, 61–64. doi:10.1016/j.mehy.2018.03.019
- Rodkvamtook, W., Kuttasingkee, N., Linsuwanon, P., Sudsawat, Y., Richards, A. L., Somsri, M., et al. (2018). Scrub Typhus Outbreak in Chonburi Province, Central Thailand, 2013. *Emerg. Infect. Dis.* 24, 361–365. doi:10.3201/eid2402.171172
- Sames, W. J., Klein, T. A., Kim, H. C., Gu, S. H., Kang, H. J., Shim, S. H., et al. (2010). Serological Surveillance of Scrub Typhus, Murine Typhus, and Leptospirosis in Small Mammals Captured at Twin Bridges Training Area, Gyeonggi Province, Republic of Korea, 2005-2007. *Mil. Med.* 175, 48–54. doi:10.7205/milmed-d-05-01308
- Seto, J., Suzuki, Y., Nakao, R., Otani, K., Yahagi, K., and Mizuta, K. (2017). Meteorological Factors Affecting Scrub Typhus Occurrence: A Retrospective Study of Yamagata Prefecture, Japan, 1984-2014. *Epidemiol. Infect.* 145, 462–470. doi:10.1017/S0950268816002430
- Sheng, F., and Jia, L. (2020). “Short-Term Load Forecasting Based on SARIMAX-LSTM,” in 2020 5th International Conference on Power and Renewable Energy (ICPRE). Presented at the 2020 5th International Conference on Power and Renewable Energy (ICPRE), Shanghai, China, September 12–14, 2020, 90–94. doi:10.1109/ICPRE51194.2020.9233117
- Sherstinsky, A. (2020). Fundamentals of Recurrent Neural Network (RNN) and Long Short-Term Memory (LSTM) Network. *Physica D: Nonlinear Phenomena* 404, 132306. doi:10.1016/j.physd.2019.132306
- Sun, Y., Wei, Y.-H., Yang, Y., Ma, Y., de Vlas, S. J., Yao, H.-W., et al. (2017). Rapid Increase of Scrub Typhus Incidence in Guangzhou, Southern China, 2006–2014. *BMC Infect. Dis.* 17, 13. doi:10.1186/s12879-016-2153-3
- Tsai, P.-J., and Yeh, H.-C. (2013). Scrub Typhus Islands in the Taiwan Area and the Association between Scrub Typhus Disease and forest Land Use and Farmer Population Density: Geographically Weighted Regression. *BMC Infect. Dis.* 13, 191. doi:10.1186/1471-2334-13-191
- Wan, R., Mei, S., Wang, J., Liu, M., and Yang, F. (2019). Multivariate Temporal Convolutional Network: A Deep Neural Networks Approach for Multivariate Time Series Forecasting. *Electronics* 8, 876. doi:10.3390/electronics8080876
- Wardrop, N. A., Kuo, C.-C., Wang, H.-C., Clements, A. C. A., Lee, P.-F., and Atkinson, P. M. (2013). Bayesian Spatial Modelling and the Significance of Agricultural Land Use to Scrub Typhus Infection in Taiwan. *Geospat Health* 8, 229–239. doi:10.4081/gh.2013.69
- Wei, Y., Huang, Y., Li, X., Ma, Y., Tao, X., Wu, X., et al. (2017). Climate Variability, Animal Reservoir and Transmission of Scrub Typhus in Southern China. *Plos Negl. Trop. Dis.* 11, e0005447. doi:10.1371/journal.pntd.0005447
- Yang, L. P., Liu, J., Wang, X. J., Ma, W., Jia, C. X., and Jiang, B. F. (2014). Effects of Meteorological Factors on Scrub Typhus in a Temperate Region of China. *Epidemiol. Infect.* 142, 2217–2226. doi:10.1017/S0950268813003208
- Yang, L.-P., Liang, S.-Y., Wang, X.-J., Li, X.-J., Wu, Y.-L., and Ma, W. (2015). Burden of Disease Measured by Disability-Adjusted Life Years and a Disease Forecasting Time Series Model of Scrub Typhus in Laiwu, China. *Plos Negl. Trop. Dis.* 9, e3420. doi:10.1371/journal.pntd.0003420
- Yao, H., Wang, Y., Mi, X., Sun, Y., Liu, K., Li, X., et al. (2019). The Scrub Typhus in mainland China: Spatiotemporal Expansion and Risk Prediction Underpinned by Complex Factors. *Emerg. Microbes Infect.* 8, 909–919. doi:10.1080/22221751.2019.1631719
- Yu, H., Sun, C., Liu, W., Li, Z., Tan, Z., Wang, X., et al. (2018). Scrub Typhus in Jiangsu Province, China: Epidemiologic Features and Spatial Risk Analysis. *BMC Infect. Dis.* 18, 372. doi:10.1186/s12879-018-3271-x
- Yu, Y., Si, X., Hu, C., and Zhang, J. (2019). A Review of Recurrent Neural Networks: LSTM Cells and Network Architectures. *Neural Comput.* 31, 1235–1270. doi:10.1162/neco\_a\_01199
- Zhang, S., Song, H., Liu, Y., Li, Q., Wang, Y., Wu, J., et al. (2010). Scrub Typhus in Previously Unrecognized Areas of Endemicity in China. *J. Clin. Microbiol.* 48, 1241–1244. doi:10.1128/JCM.01784-09
- Zhang, M., Wang, X.-J., Ding, L., Zhao, Z.-T., Li, Z., and Ding, S.-J. (2012). Scrub Typhus: Surveillance, Clinical Profile and Diagnostic Issues in Shandong, China. *Am. J. Trop. Med. Hyg.* 87, 1099–1104. doi:10.4269/ajtmh.2012.12-0306
- Zhang, W.-Y., Wang, L.-Y., Ding, F., Hu, W.-B., Soares Magalhaes, R. J., Sun, H.-L., et al. (2013). Scrub Typhus in Mainland China, 2006-2012: The Need for Targeted Public Health Interventions. *Plos Negl. Trop. Dis.* 7, e2493. doi:10.1371/journal.pntd.0002493
- Zheng, C., Jiang, D., Ding, F., Fu, J., and Hao, M. (2019). Spatiotemporal Patterns and Risk Factors for Scrub Typhus from 2007 to 2017 in Southern China. *Clin. Infect. Dis.* 69, 1205–1211. doi:10.1093/cid/ciy1050
- Zhou, X., Huang, G., Piwowar, J., Fan, Y., Wang, X., Li, Z., et al. (2018). Hydrologic Impacts of Ensemble-RCM-Projected Climate Changes in the Athabasca River Basin, Canada. *J. Hydrometeorol.* 19, 1953–1971. doi:10.1175/jhm-d-17-0232.1
- Zhou, X., Huang, G., Li, Y., Lin, Q., Yan, D., and He, X. (2021). Dynamical Downscaling of Temperature Variations over the Canadian Prairie Provinces under Climate Change. *Remote Sensing* 13, 4350. doi:10.3390/rs13214350

**Conflict of Interest:** The authors declare that the research was conducted in the absence of any commercial or financial relationships that could be construed as a potential conflict of interest.

**Publisher’s Note:** All claims expressed in this article are solely those of the authors and do not necessarily represent those of their affiliated organizations, or those of the publisher, the editors, and the reviewers. Any product that may be evaluated in this article, or claim that may be made by its manufacturer, is not guaranteed or endorsed by the publisher.

Copyright © 2022 He, Wei, Yin, Wang, Qian, Sun, Xu, Soares Magalhaes, Guo and Zhang. This is an open-access article distributed under the terms of the Creative Commons Attribution License (CC BY). The use, distribution or reproduction in other forums is permitted, provided the original author(s) and the copyright owner(s) are credited and that the original publication in this journal is cited, in accordance with accepted academic practice. No use, distribution or reproduction is permitted which does not comply with these terms.